REVIEW OF ANALYSIS OF MECHANISMS FOR EARLY WASTE PACKAGE AND DRIP SHIELD FAILURE

Prepared for

U.S. Nuclear Regulatory Commission
Contract NRC–02–07–006

Prepared by

T. Calvin Tszeng
(Consultant)

Center for Nuclear Waste Regulatory Analyses
San Antonio, Texas

September 2008

PREVIOUS REPORTS IN SERIES

Number	Name	Date Issued
CNWRA 91-004	A Review of Localized Corrosion of High-Level Nuclear Waste Container Materials—I	April 1991
CNWRA 91-008	Hydrogen Embrittlement of Candidate Container Materials	June 1991
CNWRA 92-021	A Review of Stress Corrosion Cracking of High-Level Nuclear Waste Container Materials—I	August 1992
CNWRA 93-003	Long-Term Stability of High-Level Nuclear Waste Container Materials: I—Thermal Stability of Alloy 825	February 1993
CNWRA 93-004	Experimental Investigations of Localized Corrosion of High-Level Nuclear Waste Container Materials	February 1993
CNWRA 93-006	Characteristics of Spent Nuclear Fuel and Cladding Relevant to High-Level Waste Source Term	May 1993
CNWRA 93-014	A Review of the Potential for Microbially Influenced Corrosion of High-Level Nuclear Waste Containers	June 1993
CNWRA 94-010	A Review of Degradation Modes of Alternate Container Designs and Materials	April 1994
CNWRA 94-028	Environmental Effects on Stress Corrosion Cracking of Type 316L Stainless Steel and Alloy 825 as High-Level Nuclear Waste Container Materials	October 1994
CNWRA 95-010	Experimental Investigations of Failure Processes of High-Level Radioactive Waste Container Materials	May 1995
CNWRA 95-020	Expert-Panel Review of the Integrated Waste Package Experiments Research Project	September 1995
CNWRA 96-004	Thermal Stability and Mechanical Properties of High-Level Radioactive Waste Container Materials: Assessment of Carbon and Low-Alloy Steels	May 1996
CNWRA 97-010	An Analysis of Galvanic Coupling Effects on the Performance of High-Level Nuclear Waste Container Materials	August 1997
CNWRA 98-004	Effect of Galvanic Coupling Between Overpack Materials of High-Level Nuclear Waste Containers—Experimental and Modeling Results	March 1998

PREVIOUS REPORTS IN SERIES (continued)

Number	Name	Date Issued
CNWRA 98-008	Effects of Environmental Factors on Container Life	July 1998
CNWRA 99-003	Assessment of Performance Issues Related to Alternate Engineered Barrier System Materials and Design Options	September 1999
CNWRA 99-004	Effects of Environmental Factors on the Aqueous Corrosion of High-Level Radioactive Waste Containers—Experimental Results and Models	September 1999
CNWRA 2000-06 Revision 1	Assessment of Methodologies to Confirm Container Performance Model Predictions	January 2001
CNWRA 2001-003	Effect of Environment on the Corrosion of Waste Package and Drip Shield Materials	September 2001
CNWRA 2002-01	Effect of In-Package Chemistry on the Degradation of Vitrified High-Level Radioactive Waste and Spent Nuclear Fuel Cladding	October 2001
CNWRA 2002-02	Evaluation of Analogs for the Performance Assessment of High-Level Waste Container Materials	March 2002
CNWRA 2003-01	Passive Dissolution of Container Materials—Modeling and Experiments	October 2002
CNWRA 2003-02	Stress Corrosion Cracking and Hydrogen Embrittlement of Container and Drip Shield Materials	October 2002
CNWRA 2003-05	Assessment of Mechanisms for Early Waste Package Failures	March 2003
CNWRA 2004-01	Effect of Fabrication Processes on Materials Stability —Characterization and Corrosion	October 2003
CNWRA 2004-02	Natural Analogs of High-Level Waste Container Materials—Experimental Evaluation of Josephinite	January 2004
CNWRA 2004-03	The Effects of Fabrication Processes on the Mechanical Properties of Waste Packages —Progress Report	July 2004
CNWRA 2004-08	A Review Report on High Burnup Spent Nuclear Fuel—Disposal Issues	September 2004

PREVIOUS REPORTS IN SERIES (continued)

Number	Name	Date Issued
CNWRA 2005-01	Microbially Influenced Corrosion Studies of Engineered Barrier System Materials	October 2004
CNWRA 2005-02	Passive and Localized Corrosion of Overpack Materials—Modeling and Experiments	December 2004
CNWRA 2005-03	Microstructural Analyses and Mechanical Properties of Alloy 22	March 2005
CNWRA 2006-01	Crevice Corrosion Penetration Rates of Alloy 22 in Chloride-Containing Waters—Progress Report	December 2005
CNWRA 2006-02	Corrosion of Alloy 22 in Concentrated Nitrate and Chloride Salt Environments at Elevated Temperatures —Progress Report	April 2006
CNWRA 2007-01	Stress Corrosion Cracking of Waste Package Material—Modeling and Experiments	December 2006

ABSTRACT

The U.S. Department of Energy (DOE) has determined that waste packages and drip shields will be important contributors to overall performance of a potential high-level radioactive waste repository at Yucca Mountain, Nevada (DOE, 2002). Various types of discontinuities may be introduced in a waste package or drip shield during fabrication processes (e.g., welding and heat treatment). Depending on the characteristics, some of these discontinuities may be defects that can potentially lead to early failure of the waste package or the drip shield. In a report completed under contract with DOE, Bechtel SAIC Company, LLC (2004) calculated defect characteristics using statistical analyses of existing data that are mainly related to stainless steels and materials other than Alloy 22. This early-failure analysis also includes the results of event-tree analyses to determine the probability of defective waste packages or drip shields caused by improper heat treatment, laser peening, and other procedures and processes that may involve human errors and equipment failure. Bechtel SAIC Company, LLC (2004) maintains that the flaws in the circumferential direction are not detrimental to the integrity of the waste package. Review of the DOE report (Bechtel SAIC Company, LLC, 2004) indicates that various thermal and mechanical loadings may generate stress states where principal tensile stress can be in any direction. Consequently, cracks of all orientations may be an important consideration for evaluating potential early failure. Furthermore, this review indicates that heating and cooling during heat treatment are not uniform and may be inconsistent. Therefore, the event-tree analysis may include the probability that the heating and cooling characteristics do not meet specifications. Because the operator may fail to detect or disclose waste packages that do not meet specifications, this potential human error may be an important consideration. The review includes independent calculations of the defect characteristics and event-tree analyses using a Microsoft® Office Excel (Microsoft Corporation, 2003) spreadsheet program.

References:

Bechtel SAIC Company, LLC. "Analysis of Mechanisms for Early Waste Package/Drip Shield Failure." CAL–EBS–MD–000030. Rev. 00C ICN 00. Las Vegas, Nevada: Bechtel SAIC Company, LLC. 2004.

DOE. DOE/RW–0539–1, "Yucca Mountain Science and Engineering Report-Technical Information Supporting Site Recommendation Consideration." Rev. 1. Las Vegas, Nevada: DOE. 2002.

Microsoft Corporation. "Microsoft® Office Excel 2003." Redmond, Washington: Microsoft Corporation. 2003.

Disclaimer:

This report describes work performed by the Center for Nuclear Waste Regulatory Analyses (CNWRA®) for the U.S. Nuclear Regulatory Commission (NRC) under Contract No. NRC–02–07–006. The activities reported here were performed on behalf of the NRC Office of Nuclear Material Safety and Safeguards, Division of High-Level Waste Repository Safety. This report is an independent product of CNWRA and does not necessarily reflect the view or regulatory position of NRC.

CONTENTS

FIGURES

ACKNOWLEDGMENTS

This report was prepared to document work performed by the Center for Nuclear Waste Regulatory Analyses (CNWRA®) for the U.S. Nuclear Regulatory Commission (NRC) under Contract No. NRC–02–07–006. The activities reported here were performed on behalf of the NRC Office of Nuclear Material Safety and Safeguards, Division of High-Level Waste Repository Safety. This report is an independent product of CNWRA and does not necessarily reflect the view or regulatory position of NRC.

The author gratefully acknowledges the technical reviews of D. Dunn and O. Pensado; the programmatic reviews of W. Patrick and S. Mohanty; the responses to CNWRA and NRC reviews by K. Chiang, Y.-M. Pan, and G. Adams; and the editorial reviews of E. Hansen, E. Kraus, and L. Mulverhill. He also appreciates J. Gonzalez and A. Ramos for assistance in preparing this report.

QUALITY OF DATA, ANALYSES, AND CODE DEVELOPMENT

DATA: All data identified in this report were generated by the U.S. Department of Energy (DOE).

ANALYSES AND CODES: Microsoft® Office Excel (Microsoft Corporation, 2003) was used to check all DOE-conducted calculations.

Reference:

Microsoft Corporation. "Microsoft® Office Excel 2003." Redmond, Washington: Microsoft Corporation. 2003.

EXECUTIVE SUMMARY

The U.S. Department of Energy (DOE) has determined that waste packages and drip shields will be important contributors to overall performance of a potential high-level radioactive waste repository at Yucca Mountain, Nevada (DOE, 2002). Various types of discontinuities may be introduced in a waste package or drip shield during fabrication processes (e.g., welding and heat treatment). Depending on the characteristics, some of these discontinuities may be defects that can potentially lead to early failure of the waste package or the drip shield. In a report completed under contract with DOE, Bechtel SAIC Company, LLC (2004) calculated defect characteristics using statistical analyses of existing data that are mainly related to stainless steels and materials other than Alloy 22. This early-failure analysis also includes the results of event-tree analyses to determine the probability of defective waste packages or drip shields caused by improper heat treatment, laser peening, and other procedures and processes that may involve human error and equipment failure. The review documented in this report assessed the Bechtel SAIC Company, LLC (2004) early-failure analysis of the waste package outer container and drip shield, because of manufacturing-induced defects. Although both waste packages and drip shields are considered, the discussion in this review report generally refers to waste packages for simplicity. This review focuses on weld flaws and improper heat treatment of the waste package outer container. This report reviewed the technical bases of the assumptions and their rationales related to (i) the quantification of different types of defects; (ii) the input parameters used in the analysis, (iii) the methodology and calculations used in determining the probability distributions for the expected defects before and after inspection and repair, (iv) the event-tree analysis used in determining the probability that the waste package and drip shield components are subjected to improper processes and procedures, and (v) the calculated probability distributions and parameter values used in describing the characteristics of various types of defects. All the calculations contained in the referenced report have been independently checked using a Microsoft® Office Excel (Microsoft Corporation, 2003) spreadsheet program.

Bechtel SAIC Company, LLC (2004) assumes that flaws less than 1 mm [0.039 in] will not jeopardize waste package performance and are of no importance to early failure. The flaw inspection relies heavily on the ultrasonic technique that has a threshold of about 1 mm [0.0394 in]. Furthermore, there is a dead zone for the ultrasonic inspection to detect surface defects. The appearance of near-surface defects, even though they are small, may reduce the effective threshold stress for stress corrosion cracking. The review suggests more attention be given to small defects on or near the surface. Bechtel SAIC Company, LLC (2004) maintains that flaws from insufficient fusion are in the circumferential direction and are not detrimental to the integrity of the structures. This conclusion is based mainly on the presumption that the dominant stress component that can lead to stress corrosion cracking failure is in the hoop (circumferential) direction. However, various thermal and mechanical loadings may generate stress states where principal tensile stress can be in any direction. Consequently, cracks of all orientations may be an important consideration in evaluating potential early failure. The review indicates that compressive residual stress may decrease by thermal relaxation in the waste package. Because information is unavailable on the persistence of compressive residual stress in Alloy 22, it may be prudent to consider its stability over the timeframe of interest. Furthermore, the stress state in the transition area between the peened and nonpeened regions at the surface of the welds needs to be carefully studied. This review provides independent calculations of the defect characteristics and event-tree analyses reported in Bechtel SAIC Company, LLC (2004) using Microsoft® Office Excel (Microsoft Corporation, 2003).

References:

Bechtel SAIC Company, LLC. "Analysis of Mechanisms for Early Waste Package/Drip Shield Failure." CAL–EBS–MD–000030. Rev. 00C ICN 00. Las Vegas, Nevada: Bechtel SAIC Company, LLC. 2004.

DOE. DOE/RW–0539–1, "Yucca Mountain Science and Engineering Report—Technical Information Supporting Site Recommendation Consideration." Rev. 1. Las Vegas, Nevada: DOE. 2002.

Microsoft Corporation. "Microsoft® Office Excel 2003." Redmond, Washington: Microsoft Corporation. 2003.

1 INTRODUCTION

The U.S. Department of Energy (DOE) has determined that waste packages and drip shields will be important contributors to overall performance of a potential high-level radioactive waste repository at Yucca Mountain, Nevada (DOE, 2002). The U.S. Nuclear Regulatory Commission (NRC) considers that early failures of the waste package have low significance regarding waste isolation (NRC, 2005a, Appendix D) because early failures are expected to involve only a small fraction of waste packages and do not have a significant effect on waste package performance and, consequently, on radionuclide release. However, initial defects coupled with waste package degradation processes and mechanical loading as a result of disruptive events may lead to early failures of the waste package. Disruptive events include seismic, faulting, rockfall, and dike-intrusion events. The number of waste packages that is susceptible to early-failure processes will depend on the frequency, type, size, and orientation of the initial defects.

Bechtel SAIC Company, LLC (2004) evaluated the types of defects that could occur in a waste package or a drip shield and potentially lead to its early failure and estimated a probability of occurrence for each. One acceptance criterion, established in the Yucca Mountain Review Plan, pertaining to data uncertainty regarding the degradation of engineered barriers model abstractions [NRC, 2003, Section 2.2.1.3.1.3, Acceptance Criterion 3 (4)] is applicable to the early-failure analysis of the waste package and drip shield. This acceptance criterion states

> "The DOE uses appropriate methods for nondestructive examination of fabricated engineered barriers to assess the type, size, and location of fabrication defects that may lead to premature failure as a result of rapidly initiated engineered barrier degradation. The DOE specifies and justifies the allowable distribution of fabrication defects in the engineered barriers, and assesses the effects of defects that cannot be detected on the performance of the engineered barriers."

The review documented in this report assesses the early-failure analysis of the waste package outer container and drip shield from manufacturing-induced defects presented in Bechtel SAIC Company, LLC (2004) analyses. Although both waste packages and drip shields are considered, the discussion generally refers to waste packages, for simplicity. This review focuses on weld flaws and improper heat treatment of the waste package outer container.

This report includes a review of (i) the technical bases of the assumptions and their rationales related to the quantification of different types of defects, (ii) the input parameters used in the analysis, (iii) the methodology and calculations used in determining the probability distributions for the expected defects before and after inspection and repair, (iv) the event-tree analysis used in determining the probability that the waste package and drip shield components are subjected to improper processes and procedures, and (v) the calculated probability distributions and parameter values used in describing the characteristics of various types of defects.

2 TECHNICAL REVIEW

2.1 Review of Manufacturing-Induced Defects

The Bechtel SAIC Company, LLC (2004) early-failure analysis of the waste package outer container and drip shield focused on early failure from defects induced in the stages of manufacturing and handling. The manufacturing processes considered in Bechtel SAIC Company, LLC (2004) include welding, heat treating, and laser peening. According to DOE (2002, Section 3.4.2), the basic manufacturing processes for the Alloy 22 outer cylinder include the following steps.

Offsite

- Receipt of flat plates
- Inspection for defects
- Thermally cut to dimensions
- Rolled to cylinder
- Welding (longitudinal)
- Ultrasonic inspection
- Welding preparations by machining
- Welding (circumferential)
- Ultrasonic inspection
- Stress mitigation by annealing heat treatment

Onsite

- Welding lids after loading of spent nuclear fuel rods/baskets
- Inspection for defects
- Stress mitigation by laser peening

According to DOE (2002, Section 3.4.2.5), ultrasonic inspection and other inspection methods (radiographic examination and liquid penetrant examination) would be performed on the inner and outer lid seams. However, radiographic examination does not seem to be possible for the closure lid. Penetrant examination is commonly used to detect surface defects at weld seams. If rejectable defects are found, the waste container or the waste package will need repair (Plinski, 2001). Portions of the materials would be removed and weld repair would be performed. However, defective material that cannot be satisfactorily repaired will be rejected and replaced (Plinski, 2001).

Manufacturing-induced defects are not restricted to welding, heat treatment, and laser peening. Various types of defects that can potentially lead to early failure of the waste package are reviewed in the following sections.

2.1.1 Small Defects

There is concern about defects that are too small to be detected by ultrasonic inspection. These small defects could originate from any stage of manufacturing. Some of them could exist in the raw stock material. The flaw inspection relies heavily on the technique of ultrasonic testing that has a threshold of about 1 mm [0.039 in]. The DOE document assumes that flaws smaller than 1 mm [0.039 in] will not jeopardize waste package performance and are of no

importance to early failure (Bechtel SAIC Company, LLC, 2004, p. 20). However, the mechanical and corrosion performance of waste packages may be affected by small surface defects.

First, small surface defects could lead to crack initiation and growth. For example, 50 μm [0.002 in] was recognized as the critical size for a crack to start propagation once the stress-intensity factor (K_{IC}) exceeds the threshold value (Lu, et al., 2004). Propagating cracks can coalesce, growing to where they can lead to early failure of the waste package. Indeed, Bechtel SAIC Company, LLC (2004, Section 6.4.3) points out that the formation of grain-boundary precipitates also enhances the susceptibility of the material to stress corrosion cracking. However, the small defects would need to be on the surfaces to promote stress corrosion cracking. There are various types of loading/impact that the waste package can receive in service. As a result, significant cracks can grow from these small cracks. Therefore, it may be important to consider surface defects that are smaller than 1 mm [0.039 in].

Second, the occurrence of localized corrosion as a result of small-surface defects could greatly reduce the service life and lead to early failure of the waste containers. As indicated in Bechtel SAIC Company, LLC (2004, Section 6.4.3), the improper rate of the cooling of alloys, such as Alloy 22, may result in the precipitation of carbides and intermetallic compounds along the grain boundaries. This precipitation along the grain boundaries, in turn, enhances the susceptibility of the material to localized corrosion. Small surface cracks or defects may be potential sites for localized corrosion. In fact, a longstanding concern is the critical defect size needed for localized corrosion and the density of such sites. From the corrosion standpoint, it may be important to consider surface defects that are smaller than 1 mm [0.039 in].

In summary, small surface defects that are not detectable by nondestructive examination may affect the performance of the waste package outer container and may lead to early failure.

2.1.2 Preexisting Defects

Plates produced by primary processing, such as casting or rolling, may include defects (Kapaljain and Schmid, 2002). Defects (e.g., porosity, precipitate) caused by casting are particularly common. According to Bechtel SAIC Company, LLC (2003a), one out of 19 Sierra Nuclear VSC-24 dry storage casks was found to have defects that originated from the plate-rolling process. In this case, cracks propagated along prior austenite grain boundaries of a preexisting weld.

Bechtel SAIC Company, LLC (2004, Section 4.1.4) reported that hard-alpha defects[1] are formed from very high-nitrogen or high-oxygen concentrations in the bulk titanium alloy and cannot be readily eliminated by a homogenizing heat treatment of primary mill processing (Hua, et al., 2002). These defects tend to string out during forging and rolling. Because the defects are brittle, they tend to break up during hot rolling and may form very small internal voids. Bechtel SAIC Company, LLC (2004) considers that type of defect to be one of the potential defects that could lead to early failure of the drip shield.

Although the plates for the waste package outer container would be inspected on receipt, the probability of detecting preexisting defects in the plates prior to the welding process depends on

[1]Hard-alpha defects are low-density and brittle regions of high-nitrogen or high-oxygen concentrations that occur in titanium alloys.

the defect size and location. The details of defect detection by ultrasonic inspection are given in Section 2.2.1.2 of this report.

2.1.3 Thermal Cutting and Machining for Welding Preparations

Before welding, plates will be thermally cut and machined to the required dimensions (DOE, 2002, Section 3.4.2).

Thermal Cutting

Thermal cutting imposes thermal loading and localized melting of the plate that may create microstructures near new surfaces that are different from the bulk material. For example, for Alloy 22, precipitation of carbides and intermetallic compounds can appear along the grain boundaries during cooling after thermal cutting. In practice, thermal cutting is performed along a line within a certain distance {e.g., 3.2 mm [0.12 in]} from the final dimensions. Additional machining, such as grinding, is then used to obtain the final dimensions. The concern is the assurance of complete removal of the affected zone. For greater consistency, cutting will be done only with a mechanically guided torch or a torch controlled using a guide bar, and manual cutting will not be permitted (SAC Joint Venture, 2000, Section 3.2.6).

The exact procedure of thermal cutting has not been specified in Bechtel SAIC Company, LLC (2004). Because thermal cutting may significantly affect the integrity of plate material, DOE may decide to examine the effects in greater detail.

Machining

The machining process (e.g., grinding) plastically shears the surface or edge of the plate. Both thermal cutting and machining may create locally high stresses in the plate. The thermal input from the welding process can further change the microstructure. Defects introduced during the machining or thermal-cutting processes may not be healed in the subsequent welding process.

Cleaning

Proper preparation of the weld-joint region is important in welding nickel-based alloys. A variety of mechanical and thermal-cutting methods are available to prepare weld angles. Plasma cutting/gouging, machining, grinding, and air-arc gouging are all potential processes. It is necessary to condition all thermally cut edges to bright, shiny metal before welding. The welding surface and adjacent regions should be thoroughly cleaned with an appropriate solvent before to any welding operation.

Bechtel SAIC Company, LLC (2004, Section 5.6.3) discusses the possibility of waste package contamination during cleaning. Contamination during cleaning is assumed to occur only as a result of a procedural error. It is possible that the foreign substance is not completely removed even if the procedure is strictly followed. Because contamination could compromise the weld quality, DOE may decide to closely examine the probability of contamination during cleaning and the consequence of contamination. These concerns apply to both the waste package and the drip shield.

2.1.4 Plate Rolling

Alloy 22 plates are rolled to form a cylindrical shape, followed by longitudinal welding to make the outer cylinder. The rolling processes proposed for the cylinders are widely used in many industries. However, the tolerances required for waste packages are an important aspect in the manufacturing process. The misalignments between the inner and outer cylinders of the waste package could lead to significant bend moments in the circumferential welds of the waste package as the result of local contacts.

Nonuniform plastic deformation may generate residual stress in the rolled plates. For a plate with a thickness of 20 mm [0.79 in] that is rolled to form a cylinder with a diameter of 1,524 mm [60 in], the hoop strain on the plate surface is about (20/2)/(1524/2) = 0.013. The inner and outer surfaces experience plastic deformation, and the tensile stress on the outer surface induced by bending reaches the yield stress of Alloy 22 {365 MPa [53 ksi]}. These high tensile stresses need to be relaxed in the subsequent annealing process (e.g., solution annealing) because they may promote stress corrosion cracking.

Cold rolling to form cylindrical shells will increase dislocation densities in the cold-worked regions. High-dislocation densities may create faster pathways for diffusion processes, such as phase precipitation, which could alter corrosion performance. The stress-relief heat treatment on the outer barrier and drip shield will help remove the dislocations.

DOE plans to solution anneal the fully fabricated waste package outer container to remove residual stresses before the final closure weld (Plinski, 2001). DOE should consider establishing a quality control procedure to assure stress relief by solution annealing.

2.1.5 Welding

Among the fabrication processes, welding has the greatest potential to affect the integrity of the waste package. Welding thermally and mechanically loads the structure. In addition, many factors must be considered, and the process is complex and not always consistent. The principal welding effects are on the microstructure and mechanical properties. The former relates to phases, compounds, and composition, and the latter to voids, cracks, porosity, and stress.

DOE has selected the gas metal arc and gas tungsten arc as the welding methods for the waste package (Plinski, 2001). These techniques have been successfully applied to a wide range of material systems, including nickel-chromium-molybdenum alloys and titanium alloys. Nevertheless, even when appropriate procedures are used, the completed weld may still contain defects.

Gas-metal arc welding is highly productive compared to gas-tungsten arc welding. It is well suited for both manual and automatic welding situations; however, control and ease of operation are reduced. More attention is needed in conducting gas-metal arc welding. Among the three modes of metal transfer in gas metal arc welding, short arc transfer is the most common method that is usually considered to have good weld-puddle control. However, because the process operates at low amperage, it is often regarded as a defect- (cold-lap) prone process. In comparison, gas tungsten arc welding is a very versatile, all-position welding process. The major drawback is the relatively low productivity (Haynes International, Inc., 2002).

Lack of Fusion

In the welding process, the filler metal and some of the base metal melt and solidify to form the weldment. The most common flaws for gas-metal arc and gas tungsten arc welding are insufficient fusion from a missed side wall and from the lack of penetration in the side wall. The lack of fusion can also occur between passes of a multipass weld. Flaws from the lack of fusion are usually oriented in the direction of the weld bead (i.e., oriented circumferentially, not radially, for the present cases of waste package welding). Bechtel SAIC Company, LLC (2004) maintains that the flaws from insufficient fusion are in the circumferential direction and are not detrimental to the integrity of the structures. This conclusion is based mainly on the presumption that the dominant stress component that can lead to stress corrosion cracking failure is in the hoop (circumferential) direction. Therefore, only cracks in the radial direction can be of concern. In actual situations, various thermal and mechanical loadings may generate stress states where principal tensile stresses can be in any direction. For example, the misalignment in the two cylinders and other types of distortion from stress relaxation can produce local contact stresses. The normal stress induced by bending is most likely in the longitudinal direction. In this situation, the defects oriented in the circumferential direction are a concern. Therefore, cracks of all orientations may be an important consideration for evaluating potential early failure.

Hot Cracking

Hot cracking and shrinkage porosity resulting from weld solidification in the weld for the Alloy 22 plate are not fully addressed in Bechtel SAIC Company, LLC (2004). Hot cracking is a condition generally confined to the fusion zone, but occasionally it can occur in the heat-affected zone (Haynes International, Inc., 2002). Two conditions are necessary to produce hot cracking—stress and a strain-intolerant microstructure. The creation of stress is inevitable during welding because of the complex thermal stresses that are generated when metal solidifies. Strain-intolerant microstructures temporarily occur at elevated temperatures near the melting and solidification points of all alloys. There is a low probability that the weld will be free of hot cracking. Traditionally, hot cracks and porosity can be checked by using radiographic and ultrasonic tests. DOE may consider conducting radiographic tests to identify hot cracks and porosities smaller than 1 mm [0.039 in]. The significance of small cracks is discussed in Section 2.1.1.

Moisture-Related Failure

As noted by Hodges (1998), moisture-related failure in welds has been found in dry storage casks for spent nuclear fuel. The alloy base plate may require warming to raise the temperature above freezing or to prevent moisture condensation, which may occur if the alloy is brought into a warm shop from cold outdoor storage. Moisture-related failure may not be observed in laboratory tests, because different procedures and conditions may prevail in the field. Although the specific procedure of weld preparation is not available (Bechtel SAIC Company, LLC, 2004), DOE may decide to consider removing the moisture by indirect heating immediately before welding. The possibility of moisture-related weld problems may need to be considered in the analysis of early failure.

2.1.6 Annealing by Heat Treatment

Annealing is a process in which a material is subjected to a controlled heating and cooling cycle to affect material properties. Stress-mitigation techniques, such as annealing, will be applied to

the outer cylinder to minimize the potential for stress corrosion cracking (Wong and Payer, 2002). Specifically, the main purpose of heat treatment is to relieve the residual stress induced by cold-plate rolling to form the cylinders. Heat treatment after welding can also help relieve welding-induced stresses. The details of annealing by heat treatment for the waste package are not provided in Bechtel SAIC Company, LLC (2004). Although these parameters are still being developed, DOE expects that the cylinder assembly will be heated in a furnace and then quenched by water. According to Cogar, et al. (2001), the outer cylinder will be annealed after the bottom lid has been welded and inspected. The outer cylinder will be furnace heated and held at a soak temperature of 1,121 °C ± 28 °C [2,050 °F ± 50 °F] for at least 20 minutes. Cooling will be performed by immersion in water. The cooling rate for the entire cylinder will be greater than 55.6 °C [132 °F] per minute from the soak temperature to below 371 °C [700 °F].

Heat-Treatment Variability

According to Cogar, et al. (2001), the measured stress state after annealing is predominantly compressive. However, note that quenching in immersion cooling is not a well-behaved phenomenon; large variations in the surface heat transfer coefficient are common (Tszeng and Zhou, 2004). The identical heating and quenching procedure does not provide a consistent product. Large variability in residual stress at the end of quenching is also routinely observed (Totten and Howes, 1997). Such variability may cause local residual stress to exceed the permissible average value.

Also of concern is differential cooling when the cylinder is immersed in quench water (Totten and Howes, 1997). If the cylinder is lowered into the quenching tank at a nominal speed of 300 mm/s [12 in/s] in a vertical orientation, it takes about 17 seconds to completely submerge the outer cylinder. There is a large temperature difference between the top and bottom of the cylinder. A thorough study may be necessary to quantify and evaluate the possible consequence of differential cooling and to control its effects as needed.

Variability in typical waste package and drip-shield heat-treatment processes has not been addressed in Bechtel SAIC Company, LLC (2004). The source of variability is traditionally divided into two categories: part and process. The former is represented by material composition (e.g., segregation, banding); microstructure (e.g., homogeneity, texture); prior plastic strain; surface condition; and geometry and geometrical features. The latter includes all the variables that can change during the process, primarily the heating and cooling characteristics.

The effort to relate metallurgical variability to the variability in product quality has not led to any definite conclusions (Totten and Howes, 1997). Various studies, however, have examined the influence of variability in heating and cooling on product quality (e.g., Tszeng, et al., 1996a,b). A series of studies on the quenching variability in steels and superalloys (Gamadden and Tszeng, 2001; Tszeng, et al., 1996a,b; Tszeng and Saraf, 2003; Tszeng and Zhou, 2004) indicates a strong correlation between the quenching process (even a well-controlled process) and product variability. Similar problems may occur in waste package and drip-shield materials. Because heating and cooling would not be uniform even if a waste package were heated and cooled as uniformly as possible, certain parts of the waste package would be heated or quenched at a higher rate than other locations. The nonuniformity in heating and cooling is not predictable. The high scrap rate of heat-treated parts in various industries has been partially from nonuniform heating and cooling. Based on these observations, it is important to consider that heating and cooling may affect product quality and performance.

The heat-treatment process is a critical fabrication step intended to remove any residual stresses from fabrication. The heat-treatment processes introduce compressive surface stresses to delay the onset of stress corrosion cracking. Nonuniform heating and cooling can cause formation of precipitates in the welds. These inhomogeneities are the potential sites for localized corrosion and initiation of stress corrosion cracking. Reliability can be compromised as a result of nonuniform heating and cooling.

Given the potentially large variability in heat treatment, heat-treated waste packages may need to be inspected for specification compliance. Along this line, there would be a probability that the operator fails to detect or disclose waste packages that do not meet specification. Furthermore, because such inspection needs to survey the entire waste package outer barrier, an improper inspection resulting from human error could fail to identify all the defective areas in the waste package. Therefore, an event related to heat-treatment variability may be included in the event-tree analysis for improper heat treatment to account for this type of human-reliability error.

Improper Temperature Monitoring

The assumption regarding the thermocouple installation in Bechtel SAIC Company, LLC (2004, Section 5.4.1) may not be consistent with industry practice. Although thermocouples are used to understand the heat-treatment processes in research laboratories, they are not usually used to monitor part temperature in industrial heat treatments. Proper thermocouple installation would require drilling holes into the waste package so that the actual temperature can be measured. This practice is not recommended for the waste package, because the material integrity would be compromised. Tszeng and Saraf (2003) and Tszeng and Zhou (2004) studied the effects of surface-mounted thermocouples on the measured temperatures. In-process monitoring devices (e.g., Plester, 2005) do not actually measure the part temperature; the signals only correspond to the ambient temperature in the furnace. DOE should consider verifying the process parameters using dummy specimens that are fully instrumented with either hole-drilling thermocouples or surface thermocouples. The latter is regularly used in the nuclear industry.

Generally, the temperature available to the operator for control or monitoring purposes is the furnace temperature, which is different from the part temperature. The thermocouple is built into the furnace, and there is no need for the operator to install thermocouples. Some industrial furnaces, particularly for aerospace parts, are surveyed for temperature uniformity using various temperature monitoring devices. This procedure is part of the regular furnace maintenance and not the responsibility of floor operators. Accordingly, the event-tree analysis may not include events related to thermocouple installation.

Built-in thermocouples can fail in service (e.g., the thermocouples may fail to meet the specifications if they are not calibrated according to the schedule). Because of material degradation, a thermocouple may be out of tolerance even if it is calibrated according to schedule. Thermocouple failure is different from the process malfunction, which is one of the event trees in the analysis.

2.1.7 Laser Peening

In laser peening, a high-powered laser beam produces shock waves that generate compressive stresses in the surface material. Multiple-pass laser peening can increase the depth of the compressive-stress layer. It has been shown that compressive stress can be produced at

depths of 2 to 3 mm [0.079 to 0.12 in] with multiple-pass laser peening (Bechtel SAIC Company, LLC, 2003b). Additional depth may be possible but has not been demonstrated. A shortcoming of this approach is that it only delays the potential initiation of stress corrosion cracking. Below the layer of compressive stress, the weld region may remain under tensile stress. When the compressive layer of material is lost from corrosion, the remaining material is still vulnerable to stress corrosion cracking. If the depth of compressive stress is insufficient, the performance life is reduced accordingly. Therefore, the depth of compressive stress is an important measure of the success of the laser peening.

A fully tested laser-peening process would rectify the possibility of inconsistent residual stress under the surface. Regardless, there are two concerns about the residual stress induced by laser peening: (i) relaxation of residual stress and (ii) state of stress outside the peened areas.

First, relaxation of residual stresses is frequently observed. The three primary mechanisms for residual stress relaxation are (i) tensile or compressive overload, (ii) cyclic loading, and (iii) thermal relaxation. The importance of each mechanism depends on the material and service conditions. Because no substantial tensile or compressive overload and cyclic loading are anticipated, only thermal relaxation is applicable to the waste packages.

According to Prevéy, et al. (1998), thermal relaxation progresses in two stages: a primary stage, which is extremely rapid, and a secondary stage, which appears to follow the Avrami diffusion model. Previous work by Prevéy, et al. (1998) and Prevéy and Cammett (2003) on several aerospace alloys, including Ti–6Al-4V and IN 718, found that the thermal stability of compressive residual stresses induced by mechanical surface treatments was inversely proportional to the amount of cold work. As the cold work level decreased, the thermal stability of the compressive stress state increased. For Ti–6Al–4V, laser-shock processing treatments inducing less than 5 percent cold work were found to offer good thermal stability, particularly when compared to surface treatments that induce extremely high levels of surface cold work (e.g., shot peening) (Shepard, et al., 2001).

Information on the stability of thermal stress for the Alloy 22 waste package outer container over a long period of time is not provided in Bechtel SAIC Company, LLC (2004). Although the peak temperature in the waste package is estimated to be only about 200 °C [392 °F], the relaxation of residual stress over tens or hundreds of years has not been documented. Furthermore, systematic studies of quasi-static relaxation of residual stress at higher temperatures of aerospace alloys are lacking. Without more concrete information or data, it may be prudent for DOE to evaluate the stability of residual stress induced by combined thermal and mechanical loading over the timeframe of interest.

Second, although compressive stress is expected in the peened areas, the residual tensile stress may be greater than the original, nonpeened level at the transition zone just outside the peened area. The transition area between the peened and nonpeened regions at the surface of the welds needs to be carefully studied. Numerous failures were observed at these transition regions in laser-peened steam generator tubes (Wong and Payer, 2002).

2.2 Assessment of Defect Characteristics and Failure Probabilities

This section of the review is focused on assessing the calculated probabilities and parameter values for the applicable defects discussed in Bechtel SAIC Company, LLC (2004, Section 6.2,

Mechanisms for Early Waste Package Failure; Section 6.3, Mechanisms for Early Drip Shield Failure). The main emphasis is on the weld flaws and improper heat treatment.

2.2.1 Weld Flaws

2.2.1.1 Weld Flaws in the Waste Package Before Repair

Bechtel SAIC Company, LLC (2004) cites an earlier report (Bechtel SAIC Company, LLC, 2003a) of the study on 16 weld rings of Alloy 22 that underwent the same welding procedure for the waste package outer container. Among the 16 specimens, seven flaws larger than 1 mm [0.039 in] were disclosed by the ultrasonic tests. The presence of the flaws is confirmed by the metallurgical examination.

The Bechtel SAIC Company, LLC (2004) analysis employed a chi-square test to verify that it is not unreasonable that the distribution function borrowed from studies on other material systems adequately fits the data from ultrasonic inspection. The data for weld defects are obtained from a limited experiment on 16 ring specimens reported in Bechtel SAIC Company, LLC (2003a), in which only seven flaws were found. Although the data set is small, this analysis indicated the chi-square test was successful. Thus, the basic distribution functions and parameters may fit the defect size and density with an acceptable uncertainty range (Bechtel SAIC Company, LLC, 2004).

Bechtel SAIC Company, LLC (2004) assumes that stress corrosion cracking would initiate from defects oriented in the Y-direction, which is in the through-wall direction. Therefore, only the defects in the Y-direction have been studied. The defects are characterized in several parameters: size, density, depth under the surface, and orientation. Center for Nuclear Waste Regulatory Analyses (CNWRA®) reviewed each of these parameters. The original calculations, which were performed using Mathcad®, were found to be correct.

Flaw Size

The flaw-size distribution in the Y-direction (see Bechtel SAIC Company, LLC, 2004, Figure 1) is estimated using the Bayesian approach with a noninformative prior. The reason for using the Bayesian approach, rather than the classical (also named frequentist) approach, is that it allows data updating and direct probability interpretations of the parameters to be estimated.

Bechtel SAIC Company, LLC (2004, Table 7, p.15) lists the 7 flaws found in the 16 rings. There were two 1.6-mm [0.062-in] flaws, three 3.2-mm [0.12-in] flaws, one 4.8-mm [0.19-in] flaw, and one 14.3-mm [0.56-in] flaw. The cumulative flaw-size distribution, $P_{sg}(s,\lambda_s,t)$, in the Y-direction of a weld of thickness, t (mm), is assumed to follow the normalized exponential distribution

where

$$P_{sg}(s,\lambda_s,t) = \frac{1 - e^{-\lambda_s s}}{1 - e^{-\lambda_s t}} \tag{2-1}$$

s — flaw size
λ_s — flaw-size parameter

The flaw-size parameter is determined by the Bayesian approach with a noninformative prior. The Bayesian estimation consists of updating the analyst's belief about the parameter with evidence from observation to obtain a posterior distribution. The Bayesian approach uses a probability distribution on the parameter to be estimated to express confidence. This has been a common way for NRC to represent uncertainty (NRC, 1975). Using a noninformative prior distribution has the advantage of generating the posterior estimate that minimizes the relative importance of the prior distribution compared to the data. The Bechtel SAIC Company, LLC (2004) analysis assumed that the flaw size reported in Bechtel SAIC Company, LLC (2003a) is characterized as gamma sampling. The probability density function of the flaw-size parameter is

$$p_{\lambda s}(\lambda_s) = \frac{s_t^{n_f}}{\Gamma(n_f)} \lambda_s^{n_f - 1} e^{-\lambda_s s_t} \tag{2-2}$$

where

Γ — gamma function
s_t — sum of all flaws {= 31.75 mm [1.25 in] for the present study}
n_f — number of flaws (= 7 in the present study)

Bechtel SAIC Company, LLC (2004, Figure 3) shows the calculated cumulative-distribution function on the flaw size. The calculations were carried out on Mathcad, and the data are given in Attachment I. The 5th and 95th percentiles of the flaw parameters are calculated in Eqs. (4) and (5) of the document. In Mathcad, the values are actually calculated by using the inverse cumulative-probability-distribution function DCHISQ with a degree of freedom of 14. CNWRA found the calculations correct. CNWRA also checked the cumulative-distribution function on flaw size by using the classical approach. The maximum-likelihood estimator of the flaw parameter λ_s was found to be the same as the posterior mean that is given by $\lambda_{sm} = n_f/s_t$. By using the data of the present study, it was found that λ_{sm} = 0.22/mm [5.6/in]. By using the maximum-likelihood estimator of the flaw parameter λ_s in Eq. (2-1), the cumulative-distribution function was calculated and is shown in Figure 2-1. The results are essentially identical to those using the Bayesian approach. The minor differences are attributable to the approximate nature of calculation by a maximum-likelihood estimator. This comparison confirms the reported calculations.

The information provided in Bechtel SAIC Company, LLC (2004, Table 7) is based on the data originally reported in Bechtel SAIC Company, LLC (2003a). These flaw sizes were obtained by an ultrasonic technique that has a best sensitivity of about 1 mm [0.039 in]. The smallest flaw size in the Y-direction reported in Bechtel SAIC Company, LLC (2003a) is 1.6 mm [0.062 in].

Thus, the resulting distribution function of flaw size is actually truncated at 1 mm [0.039 in]; the flaw-size distributions in Figure 2-1 have been extended to zero.

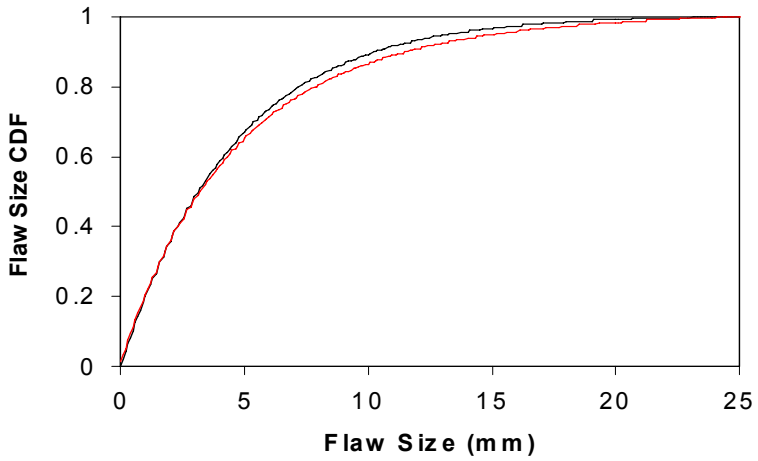

Figure 2-1. Cumulative-Distribution Function for Flaw Size Before Ultrasonic Inspection in Outer Lid Weld. There Are Two Curves in the Figure: One From Bechtel SAIC Company, LLC (2004) and the Other From the Present Calculation.

To verify that it is not unreasonable that P_{sg} of Eq. (2-1) adequately fits the data from ultrasonic inspection, the document used a chi-square test using λ_{sm} as the flaw-size parameter and t = 25 mm [0.98 in]. The test states that the assumed fitting is not unreasonable if the Pearson statistic, χ^2, is smaller than the 95th percentile of the chi-square distribution with (M−1−1) degree of freedom, $\chi^2_{0.95}$ (M−1−1)

$$\chi^2 = \sum_i^M \frac{(N_i - np_i)^2}{np_i} < \chi^2_{0.95}(M-1-1) \tag{2-3}$$

where

χ^2 — chi-square statistic (also called Pearson statistic)
M — number of cells into which the empirical data are partitioned
ρ_i — probability that a random observation falls into cell i (i varies from 1 to M)
n — total number of empirical data (for the flaw-size data, $n = n_f$)
N_i — number of empirical data that fall into cell i

The data were divided into three cells (M = 3), whose probabilities were found to be about equal (33 percent). The calculated values were χ^2 = 2 and $\chi^2_{0.95}$ (M − 1 − 1) = 3.84.

Flaw Density

The flaw-density distribution in the weld was similarly estimated using the Bayesian approach. Given a weld length, L (m), and a flaw-density parameter, λ_d, Bechtel SAIC Company, LLC (2004) uses a Poisson distribution to characterize the probability of the number of flaws, n

$$P_n\ (n, \lambda_d, L) = e^{-\lambda_d L} \frac{(\lambda_d L)^n}{n!} \tag{2-4}$$

The resulting posterior-probability density function of the flaw-density parameter is given in Bechtel SAIC Company, LLC [(2004, Eq. (12)], and the calculated flaw density is summarized in Bechtel SAIC Company, LLC (2004, Table 13). The results give the probability per outer lid weld to have zero flaws as 0.63, one flaw as 0.29, and two or more flaws as 0.08. CNWRA confirmed these calculations and, as a secondary check, CNWRA used the classical approach to determine the flaw density. According to the maximum-likelihood estimator of the flaw-density parameter, the posterior mean, λ_{dm}, is

$$\lambda_{dm} = \frac{2n_f + 1}{2L_t} \tag{2-5}$$

where L_t is the total length of the weld {= 4.85 m [15.9 ft] × 16 = 77.60 m [254.6 ft]}. The value of λ_{dm} is determined to be 0.097 flaw/m [0.029 flaw/ft]. By using Eq. (2-3) with parameters L_t = 4.85 m [15.9 ft] (single specimen) and λ_d = 0.097, the probability to have zero flaws is 0.63, one flaw is 0.29, and two or more flaws is 0.08. These results are identical to those obtained by the Bayesian approach as reported in Bechtel SAIC Company, LLC (2004, Table 13). The reported flaw density is comparable to that obtained on welded stainless steel (Khaleel, et al., 1999). According to Khaleel, et al. (1999), the flaw density for a welded pipe with a 25.4-mm [1-in] wall thickness is 1.8 flaw/m [0.55 flaw/ft]. This datum was obtained using their RR-PRODIGAL flaw distribution model. Bechtel SAIC Company, LLC (2004) reports 0.097 flaw/m [0.029 flaw/ft] in the welds of the waste package.

Depth of Flaws

Bechtel SAIC Company, LLC (2004) assumes uniform spatial distribution of flaws in the weld. To verify that a uniform distribution is not unreasonable to represent flaw depths, a chi-square test was performed at the 0.05 significance level. CNWRA confirmed the conclusion that using a uniform distribution to estimate the flaw-depth distribution does not contradict the data.

Flaws Orientation

In Bechtel SAIC Company, LLC (2004, Section 6.2.1.1.4), the probability-density function of flaw orientation is assumed to follow a normal distribution whose cumulative-distribution function is

$$P_\theta(\theta,\sigma) = 2\int_0^\theta \frac{1}{\sigma\sqrt{2\pi}} exp\left[-\frac{1}{2}\left(\frac{u}{\sigma}\right)^2\right] du \tag{2-6}$$

The standard deviation, σ, of the normal distribution is evaluated using the Bayesian approach with a noninformative prior. Based on the seven flaws reported by Bechtel SAIC Company, LLC (2004, Table 7), the mean and 95th-percentile standard variation are determined to be 13.9° and 21.6°, respectively. Based on previous developments, the expected fraction of flaws, F_θ, that has an angle θ greater than 45° is calculated as

$$F_\theta = \int_0^\infty [(1 - P_\theta(\theta,\sigma)]\, p(\sigma) d\sigma \tag{2-7}$$

Bechtel SAIC Company, LLC (2004) reports that the fraction of flaws that have an angle, θ, greater than 45° is 0.8 percent. CNWRA found the calculation in the relevant part of

Attachment I to be correct. Additional confirmation of the calculation can be established by using the mean value of the standard deviation, σ_m, in Eqs. (2-5) and (2-6). In this case, $F_\theta \approx 1 - P_\theta(\theta,\sigma_m)$. The calculated fraction of flaws with angles, θ, greater than 45° is 0.12 percent, which is in the same order of magnitude of the reported value of 0.8 percent. Using the mean and 95th-percentile standard variation, the fraction of flaws having an angle greater than a certain value was calculated (Figure 2-2). At the 95th percentile, 3.7 percent of flaws have angles greater than 45°. Overall, CNWRA confirmed the conclusion that almost all the flaws are in the direction of the weld. Flaws that are radially oriented (i.e., making an angle of 45° or more with respect to the direction of the weld) represent less than a median value of 1 percent of the total.

2.2.1.2 Weld Flaws in Waste Package After Inspection and Repair

DOE will perform ultrasonic inspection to detect and repair the flaws that may adversely affect waste package performance (Plinski, 2001). Therefore, the effectiveness of repair depends primarily on the characteristics of ultrasonic inspection.

Probability-of-Nondetection Curves of Ultrasonic Inspection

The reliability of the ultrasonic technique is characterized by the probability of nondetection, which depends on factors such as defect size, depth under the surface, material, operator skill and experience, and so on. Because the probability-of-nondetection curve for ultrasonic inspection of waste package sections has not been developed, DOE uses the Bush equation (Bush, 1983) to describe the probability of nondetection of a flaw as a function of its size. Bechtel SAIC Company, LLC (2004) claims that the ultrasonic probability-of-nondetection curves shown by Bechtel SAIC Company, LLC (2004, Figure 6) indicate less detection

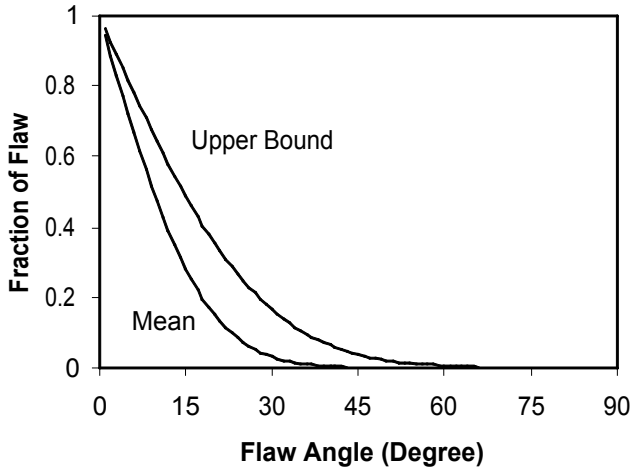

Figure 2-2. The Fraction of Flaws That Have an Angle Greater Than a Certain Value. The Two Curves Correspond to the Mean and 95th Percentile (Close to the Upper Bound).

capability than what is attainable on waste package closure welds using current industry equipment. Although the probability of nondetection is conservative in view of the advance of current ultrasonic technology, there is a significant difference between in-service (shop floor) and laboratory measurements (Doctor and Spanner, 1993). The former may have time and operating condition constraints that are absent in the laboratory. All factors considered, the probability-of-nondetection curves in Bechtel SAIC Company, LLC (2004, Figure 6) may be appropriate.

The Bush equation [Bechtel SAIC Company, LLC, 2004, Eq. (21)] does not include the dependence on the depth of the flaws beneath the surface. The conventional pulse-echo ultrasonic technique is not reliable in detecting flaws on the surface and just under the surface. Consequently, the probability of nondetection increases rapidly as the depth approaches zero (surface), increasing the potential to underestimate flaw density. Raleigh wave technique is more effective in detecting surface or subsurface flaws. If the Raleigh wave technique is not used in waste package inspection, defects on or near the surface may not be detected. The consequence is that the nondetected surface or near-surface flaws will stay in the waste package without repair and may lead to early failure. Further evaluating the reliability of the ultrasonic techniques may be an important consideration.

Flaw Size Distribution

The probability-of-nondetection curve in Bechtel SAIC Company, LLC [2004, Eq. (21)] was used in combination with the flaw-size-distribution function to determine the flaw-size distribution after ultrasonic inspection and weld repair. CNWRA checked the calculations and found them correct.

Flaw Density

The probability-of-nondetection curve in Bechtel SAIC Company, LLC [2004, Eq. (21)] was used in combination with the distribution function for the flaw-density parameter to determine the flaw-density distribution after ultrasonic inspection and weld repair. The mean flaw-density, λ_{mdut}, was calculated to be 4.1×10^{-2} flaw/m [1.2×10^{-2} flaw/ft] in the weld. CNWRA checked the calculations and found them correct.

Flaw Depth and Orientation

The repair of weld flaws would affect the flaw depth distribution and flaw orientation. At the very least, the flaw depth distribution would no longer be uniform. Based on the conservative approach, the results reported by Bechtel SAIC Company, LLC (2004, Sections 6.2.1.1.3 and 6.2.1.1.4) appear to be appropriate to characterize the flaw depth distribution and the flaw orientation in the closure welds that have been inspected and repaired.

In view of the decreasing probability of detection for surface and near-subsurface flaws by ultrasonic inspection, more near-surface flaws could remain after repairs. These flaws are detrimental to the service life of the waste package if the flaw size exceeds the depth of the compressive layer or if the flaw is located in a transition zone at the edge of the laser-peened region.

2.2.2 Base-Metal Flaws

Because the base metal would have been fully inspected and repaired before being fabricated into waste packages, Bechtel SAIC Company, LLC (2004) assumed that flaws in the base metal are initiated by an error of the welder performing a base-metal repair. The failure of the welder to use the written procedure governing the repairs to base metal can be represented by the human-error probability (HEP)[2] for failing to follow a written procedure under normal operating conditions. The HEP is assumed to follow lognormal distributions and is estimated at 0.01 (median) with an error factor of 3. The failure of the checker to detect the errors made by the welder is estimated at 0.1 (median) with an error factor of 5. Based on Bechtel SAIC Company, LLC [2004, Eqs. (35)–(38)], the mean, F_{bm}, for the frequency of occurrence of base metal flaws after repairs was calculated as $F_{bm} = 2.0 \times 10^{-3}$ per waste package. CNWRA found the calculation correct.

Similar to Eq. (2-4), the Poisson distribution is assumed to characterize the probability on the number of flaws, n

$$P_{nbm}(n, \lambda_{bm}, V_{rbm}) = e - \lambda_{bm} V_{rbm} \frac{(\lambda_{bm} V_{rbm})^n}{n!} \tag{2-8}$$

where λ_{bm} is the mean-flaw density of base metal and V_{rbm} is the volume of repaired base metal in a waste package. The cumulative-distribution function on the numbers, n, of base-metal flaws in the Alloy 22 barrier of a waste package is

$$P_{nbm}(n, \lambda_{bm}, V_{rbm}) = (1 - F_{bm}) + F_{bm} e^{-I_{bm} V_{rbm}} \sum_{i=0}^{n} \frac{(\lambda_{bm} V_{rbm})^i}{i!} \tag{2-9}$$

The cumulative-distribution function of having zero flaws is

$$P_{nbm}(0, \lambda_{bm}, V_{rbm}) = (1 - F_{bm}) + F_{bm} e - \lambda_{bm} V_{rbm} \approx (1 - F_{bm}) + F_{bm}(1 - \lambda_{bm} V_{rbm}) = 1 - F_{bm} \lambda_{bm} V_{rbm} \tag{2-10}$$

The approximation is because $\lambda_{bm} V_{rbm}$ is very small. Therefore, the probability of having at least one flaw in the base metal of a randomly selected waste package is

$$F = 1 - P_{nbm}(0, \lambda_{bm}, V_{rbm}) \approx F_{bm} \lambda_{bm} V_{rbm} \tag{2-11}$$

Bechtel SAIC Company, LLC (2004) assumes that the repaired base metal has a surface area of 100 cm^2 [15 in^2] and a thickness of 2 cm [0.79 in]. Therefore, the repair volume is $V_{rbm} = 2.0 \times 10^{-4}$ m^3 [7.1×10^{-3} ft^3]. The mean flaw-density of base metal, λ_{bm}, is assumed to be one-eighth of that corresponding to an inspected and repaired weld, which is calculated to be 4.1×10^{-2} flaw/m [1.2×10^{-2} flaw/ft] in the weld. The cross-sectional area of the weld is 2.4×10^{-4} m^2 [2.6×10^{-3} ft^2]. Therefore, the volumetric-flaw density of the weld is 1.7×10^2 flaw/m^3 [4.8 flaw/ft^3]. The mean flaw-density of base metal, λ_{bm}, is $(1.7 \times 10^2)/8 = 21$ flaw/m^3 [0.6 flaw/ft^3]. CNWRA found the calculations by Bechtel SAIC Company, LLC (2004, Attachment I) to be correct. With these numbers, the approximate probability that a waste package has at least one base-metal flaw after inspection and repair is

[2]Human-error probability is referenced frequently throughout this section; therefore, the acronym HEP will be used.

calculated $F = (2.0 \times 10^{-3})\ [(1.7 \times 10^{2})/8]\ (2.0 \times 10^{-4}) = 8.6 \times 10^{-6}$ per waste package. Again, CNWRA found the calculations correct.

2.2.3 Improper Heat Treatment

SAPHIRE software was used to calculate the probability that waste packages may undergo improper heat treatment. Each of the seven events was assigned a HEP with median-value and error factors that were mainly adopted from the technique of the human-error rate prediction (THERP)[3] method developed by Swain and Guttmann (1983). These data are recommended for use by NRC (1983, Sections 4.1 and 4.5.7) to evaluate the probability of occurrence of human errors for risk assessments for nuclear power plants. This section includes both an analysis of the event sequences and a discussion on the use of human-reliability analysis (HRA)[4] methods for the improper heat treatment of waste packages.

It is not clear that it is appropriate to use THERP (Swain and Guttmann, 1983) as the HRA method to obtain HEP. Stating that THERP has been used in other industries does not provide an adequate technical basis on its own. The HRA supporting the error probabilities may follow [e.g., the general HRA good practices in NRC (2005b, 2006)].[5] In addition, NRC (2006) for example, may be consulted for general guidance regarding the appropriate use and/or application of THERP (or other HRA methods). For instance, NRC (2006) cautions that error probabilities from THERP tables should not be applied without a proper underlying task analysis:

> "It should be noted that the tables of nominal HEPs in Chapter 20 of NUREG/CR–1278 are susceptible to being applied directly to human-failure events in the probabilistic risk assessment model without careful consideration of plant-specific performance-shaping factors dependence, and other factors. Such short-cut applications of THERP obviate the qualitative insights to be gleaned from a proper task analysis (such qualitative insights are a principal strength of HRA), and cannot be considered valid, as they clearly violate the precepts stated by the authors of THERP (NRC, 2006, p. 3-2)."

The mean probability of each event was calculated by using Bechtel SAIC Company, LLC [2004, Eq. (36)], and the results are shown in Bechtel SAIC Company, LLC (2004, Table 14). CNWRA found the calculations correct. The actual event-tree analysis of the improper heat treatment was conducted by using the SAPHIRE software. Monte Carlo sampling was carried out to determine the resultant probability. The resulting mean probability of improper heat treatment was 2.7×10^{-5} per waste package. By using the data of Bechtel SAIC Company, LLC, (2004, Attachment II) in an electronic file, waste package fault and event-trees.sra, CNWRA was able to examine the calculations reported in the document. The calculated results of improper heat treatment for the waste package were 1.6×10^{-5} per waste package (frequency) and 2.7×10^{-5} per waste package (mean probability). The calculations considered that two components (outer lid and outside barrier) were subjected to improper heat treatment. According to Bechtel SAIC Company, LLC (2004, p. 74), the waste package outer bottom lid and the outer barrier were considered in the analysis. Because the bottom lid was welded before the waste was placed in the container, it was heat-treated together with the outer barrier.

[3]Technique of human-error rate prediction is used frequently throughout this section; therefore, the acronym THERP will be used.
[4]Human-reliability analysis is used frequently throughout this section; therefore, the acronym HRA will be used.
[5]Although NUREG–1792 (NRC, 2005b) and NUREG–1842 (NRC, 2006) were developed for internal events at nuclear power plant operations, they provide general guidance for other applications also.

The results for the drip shield (one heat-treated component) were 7.9×10^{-6} per drip shield (frequency) and 1.3×10^{-5} per drip shield (mean probability). CNWRA used a simple calculation to determine the approximate frequency of improper heat treatment. According to Bechtel SAIC Company, LLC (2004, Figure 9, event-tree diagram), the highest probability of improper heat treatment is caused by event sequence #12, which involves the following four events: (i) operator chooses incorrect heat treatment/quenching program, (ii) waste package thermocouples are improperly installed, (iii) checker does not recover technician's mistake, and (iv) checker does not recover operator's mistake. Using the mean-probability values in Table 14 of Bechtel SAIC Company, LLC (2004), the frequency for event sequence #12 was estimated by

$F = (3.75 \times 10^{-3}) (8.07 \times 10^{-2}) (1.61 \times 10^{-1}) (1.61 \times 10^{-1}) = 7.84 \times 10^{-6}$ per waste package.

The calculated frequency of improper heat treatment corresponds to a single component. This calculation is very close to the full Monte Carlo calculations of Bechtel SAIC Company, LLC (2004), confirming reasonableness of the calculations.

As mentioned in Section 2.1.6, however, the event related to thermocouple installation may not be included in the analysis. Further, the possibility of a large effect from material variability and process controls (particularly quenching) may be considered in the analysis.

If the event related to thermocouple installation is removed from the analysis, the most probable improper heat treatment could be the result of the following sequence of events:

- Operator fails to select correct heat-treatment/quenching program
- Checker fails to detect that operator chose incorrect heat-treatment/quenching program

The frequency of improper heat treatment for the waste package with two heat-treated components is estimated by $F = 2 \times (3.75 \times 10^{-3}) (1.61 \times 10^{-1}) = 1.21 \times 10^{-3}$ per waste package.

This is about two orders of magnitude greater than the one previously estimated. Because of this high rate of improper heat treatment, DOE should consider further study of this matter.

Also of concern is the difficulty in using data related to human reliability. Gertman, et al. (2001) found that human performance contributed significantly to analyzed events, with latent errors (i.e., errors committed before the event whose effects are not discovered until an event occurs) being four times more prevalent than active errors (i.e., those occurring during event response). The latent errors included failures to correct known problems and errors committed during design, maintenance, and operations activities. The results of that study indicate that the underlying models of dependency in human reliability analysis may warrant further attention. As far as improper heat treatment is concerned, residual stress excessively higher than average can appear in the waste package because of the large variability of the quenching process. If such variability is not well quantified and confined in the stage of process development, it can lead to latent error.

The data uncertainty was handled approximately in the approach of Bechtel SAIC Company, LLC (2004). According to the calculations, the most probable improper heat treatment is the result of the following sequence of events:

- Operator fails to select correct heat treatment/quenching program
- Checker fails to detect that operator chose incorrect heat treatment/quenching program

- Technician fails to properly install the waste package thermocouples
- Checker fails to detect that waste package thermocouples were improperly installed

The assumed HEP for checking is 1.61×10^{-1}. In the case of a twice higher mean HEP (median = 0.2 and error factor = 7.5), the improper heat treatment rises to 1.08×10^{-4} per waste package (mean probability), which is still within the 95th percentile (1.10×10^{-4} per waste package).

3 SUMMARY

This review assessed the Bechtel SAIC Company, LLC (2004) early-failure analysis of the waste package outer container and drip shield caused by manufacturing or handling-induced defects. It focused on weld flaws and improper heat treatment. This assessment reviewed (i) the technical bases of the assumptions and their rationales related to the quantification of different types of defects, (ii) the input parameters used in the analysis, (iii) the methodology and calculations used in determining the probability distributions for the expected defects before and after inspection and repair, (iv) the event-tree analysis used in determining the probability that the waste package and drip shield components are subjected to improper processes and procedures, and (v) the calculated probability distributions and parameter values used to describe the characteristics of various types of defects.

The main findings include the following:

- Defects can be induced in several stages in waste package manufacturing that were not addressed in Bechtel SAIC Company, LLC (2004). These stages include thermal cutting and machining for welding preparations, and plate rolling.

- Bechtel SAIC Company, LLC (2004) did not address potential effects from thermal cutting. Because thermal cutting has a potentially large effect on the integrity of the plate material, there may be a need to examine the effects in greater detail. Similar concerns have been raised regarding the machining process (e.g., grinding), which imposes severe plastic shearing on the machined surface or edge of the plate. Both thermal cutting and machining could create locally high stresses in the plate.

- Flaw inspection discussed by DOE relies heavily on the ultrasonic technique, which has a threshold of about 1 mm [0.039 in]. Bechtel SAIC Company, LLC (2004) assumes that flaws smaller than 1 mm [0.039 in] will not jeopardize waste package performance and are of no importance to early failure. From the standpoint of either crack growth or localized corrosion, failing to address surface defects smaller than 1 mm [0.039 in] may not be well justified.

- The DOE analysis maintains that flaws from insufficient fusion are in the circumferential direction and are not detrimental to the integrity of the structures. This conclusion is based mainly on the presumption that the dominant stress component that can lead to stress corrosion cracking failure is in the hoop (circumferential) direction. However, various thermal and mechanical loadings may generate stress states in which principal tensile stress can be in any direction. Consequently, cracks of all orientations may be an important consideration for evaluating potential early failure.

- The occurrence of hot cracking and shrinkage porosity in the weld for the Alloy 22 plate may need to be addressed in the analysis. This possibility of a moisture-related weld problem may need to be considered for inclusion in the analysis of early-failure.

- Nonuniformity and variability in typical heat-treatment processes are of concern. Given the typically large variability in heat treatment, the heat-treated waste package may need to be inspected for specification compliance. There is a possibility that the operator fails to detect or disclose waste packages that do not meet specifications. Although thermocouples are used to understand the heat-treatment processes in research laboratories, they are not usually used to monitor part temperature in industrial heat

treatments. Accordingly, the event-tree analysis may not include the event related to thermocouple installation for monitoring part temperature.

- The review indicates that compressive residual stress may decrease by thermal relaxation in the waste packages. Because information is not provided on the persistence of compressive residual stress in Alloy 22, it may be prudent for DOE to consider its stability over the timeframe of interest. Furthermore, the stress state in the transition area between the peened and nonpeened regions at the surface of the welds may need to be carefully studied.

- The review provides independent calculations of the defect characteristics originally reported by Bechtel SAIC Company, LLC (2004, Attachment I). The original calculations, which were performed by using Mathcad, appeared to be appropriate.

4 REFERENCES

Bechtel SAIC Company, LLC. "Analysis of Mechanisms for Early Waste Package/Drip Shield Failure." CAL–EBS–MD–000030. Rev. 00C ICN 00. Las Vegas, Nevada: Bechtel SAIC Company, LLC. 2004.

———. "Repository Design Project, RDP/PA IED Typical Waste Package Component Assembly (6)." 800–IED–WIS0–00206–000–00A. Las Vegas, Nevada: Bechtel SAIC Company, LLC. 2003a.

———. "Technical Basis Document No. 6: Waste Package and Drip Shield Corrosion." Rev. 1. Las Vegas, Nevada: Bechtel SAIC Company, LLC. 2003b.

Bush, S.H. NUREG/CR–3110, "Reliability of Nondestructive Examination." Vol. 3. Washington, DC: NRC. 1983.

Cogar, J.A., W.J. DeCooman, and M. Plinski. "Waste Package Fabrication and Closure-Weld Development for the Yucca Mountain Project–GFY 2000." Proceedings of WM2001 Conference, Tucson, Arizona, February 25–March 1, 2001. Tucson, Arizona: WM Symposium, Inc. 2001.

Doctor, S.R. and J.C. Spanner, Sr. "Studies on the Quantification of NDE Reliability." *ASME PVP–257: Scientific and Engineering Aspects of Nondestructive Evaluation*. New York City, New York: American Society of Mechanical Engineers. pp. 39–46. 1993.

DOE. DOE/RW–0539–1, "Yucca Mountain Science and Engineering Report—Technical Information Supporting Site Recommendation Consideration." Rev. 1. Las Vegas, Nevada: DOE. 2002.

Gamadden, K. and T.C. Tszeng. "An Integrated Approach to Estimate the Surface Heat Transfer Coefficients in Heat Treating Processes." Proceedings of ASM International/IFHTSE Symposium on Quenching and Control of Distortion, Indianapolis, Indiana, October 5–8, 2001. (Published on CD-ROM). Materials Park, Ohio: ASM International. 2001.

Gertman, D.I., B.P. Hallbert, M.W. Parrish, M.B Sattision, D. Brownson, and J.P. Tortorelli. "Review of Findings for Human Error Contribution to Risk in Operating Events." INEEL/EXT-01–01166. Washington, DC: NRC. 2001.

Haynes International, Inc. "Fabrication of Haynes and Hastelloy Solid-Solution-Strengthened High-Temperature Alloys." Kokomo, Indiana: Haynes International, Inc. 2002.

Hodges, M.W. "Confirmatory Action Letter 97–7–001, Technical Evaluation." Docket No. 72-1007. Washington, DC: NRC. 1998.

Hua, F., J.S.J. Jevec, and G. Gordon. "General Corrosion Studies of Candidate Container Materials in Environments Relevant to Nuclear Waste Repository." Proceedings of CORROSION 2002 Conference. Paper No. 02530. Houston, Texas: NACE International. 2002.

Kapaljain, S. and S. Schmid. *Manufacturing Processes for Engineering Materials*. 4th edition. Upper Saddle River, New Jersey: Prentice Hall. 2002.

Khaleel, M.A., O.J.V. Chapman, D.O. Harris, and F.A. Simonen. "Flaw-size Distribution and Flaw Existence Frequencies in Nuclear Piping." *ASME PVP–386: Probabilistic and Environmental Aspects of Fracture and Fatigue*. New York City, New York: American Society of Mechanical Engineers. pp. 127–144. 1999.

Lu, S.C., G.M. Gordon, and P.L. Andresen. "Validation of Stress Corrosion Cracking Model for High Level Radioactive-Waste Packages." *ASME PVP-483: Transportation, Storage, and Disposal of Radioactive Materials*. New York City, New York: American Society of Mechanical Engineers. pp. 61–68. 2004.

NRC. NUREG–1842, "Evaluation of Human Reliability Analysis Methods Against Good Practices." Washington, DC: NRC. 2006.

———. NUREG–1762, "Integrated Issue Resolution Status Report." Rev. 1. Washington, DC: NRC. 2005a.

———. NUREG–1792, "Good Practices for Implementing Human Reliability Analysis (HRA)." Washington, DC: NRC. 2005b.

———. NUREG–1804, "Yucca Mountain Review Plan." Rev. 2. Washington, DC: NRC. 2003.

———. NUREG/CR–2300, "PRA Procedures Guide, A Guide to the Performance of Probabilistic Risk Assessment for Nuclear Power Plants." Washington, DC: NRC. 1983.

———. "Reactor Safety Study: An Assessment of Accident Risks in U.S. Commercial Nuclear Power Plants." WASH–1400. Washington, DC: NRC. 1975.

Plester, D. "In-Process Monitoring Equipment in Heat Treatment Today." *Industrial Heating*. March 2005. <http://www.industrialheating.com/CDA/ArticleInformation/features/BNP Features Item/0,2832,146319,00.html>. (April 12, 2005).

Plinski, M.J. "Waste Package Operations Fabrication Process Report." TDR–EBS–ND–000003. Rev. 2. Las Vegas, Nevada: Bechtel SAIC Company, LLC. 2001.

Prevéy, P. and J.T. Cammett. "The Effect of Shot Peening Coverage on Residual Stress, Cold Work and Fatigue in a Ni-Cr-Mo Low Alloy Steel." Proceedings of the 8th International Conference on Shot Peening. Weinheim, Germany: Wiley-VCH. pp. 295–304. 2003.

Prevéy, P., D. Hornbach, and P. Mason. "Thermal Residual Stress Relaxation and Distortion in Surface Enhanced Gas Turbine Engine Components." Proceedings of the 17th Heat Treating Society Conference and Exposition and the 1st International Induction Heat Treating Symposium. Materials Park, Ohio: ASM International. pp. 3–12. 1998.

SAC Joint Venture. "Recommended Specifications and Quality Assurance Guidelines for Steel Moment-Frame Construction for Seismic Applications." FEMA–353. Washington, DC: Federal Emergency Management Agency. 2000.

Shepard, M.J., P.R. Smith, and M.S. Amer. "Introduction of Compressive Residual Stresses in Ti–6Al–4V Simulated Airfoils via Laser Shock Processing." *Journal of Materials Engineering and Performance*. Vol. 10. pp. 670–678. 2001.

Swain, A.D. and H.E. Guttmann. NUREG/CR–1278, "Handbook of Human Reliability Analysis With Emphasis on Nuclear Power Plant Applications Final Report." Washington, DC: NRC. 1983.

Totten, G.E. and M.A.H. Howes. *Steels Heat Treatment Handbook*. New York City, New York: Marcel and Dekker, Inc. 1997.

Tszeng, T.C. and V. Saraf. "A Study of Fin Effects in the Measurement of Temperature Using Surface Mounted Thermocouples." *Journal of Heat Transfer*. Vol. 125. pp. 926–935. 2003.

Tszeng, T.C. and G.F. Zhou. "A Dual-Scale Computational Method for Correcting Surface Temperature Measurement Errors." *Journal of Heat Transfer*. Vol. 126. pp. 535–539. 2004.

Tszeng, T.C., W.T. Wu, and J.P. Tang. "Prediction of Distortion During Heat Treating and Machining Processes." Proceedings of the 16th ASM Heat Treating Society Conference and Exposition. Materials Park, Ohio: ASM International. pp. 9–15. 1996a.

Tszeng, T.C., W.T. Wu, and L. Semiatin. "A Sensitivity Study of the Process Models for Predicting the Distortion During Heat Treating." Proceedings of the 2nd International Conference on Quenching and Control of Distortion. Materials Park, Ohio: ASM International. pp. 321–328. 1996b.

Wong, F.M.G. and J.H. Payer, eds. "Waste Package Materials Performance Peer Review—A Compilation of Special Topic Reports." Las Vegas, Nevada: DOE. 2002.

APPENDIX

REVIEW CALCULATIONS USING MICROSOFT® OFFICE EXCEL FILES

REVIEW CALCULATIONS USING MICROSOFT® OFFICE EXCEL FILES

1 FLAW SIZE (EXCEL FILES A1.XLS AND A2.XLS)

The cumulative-flaw-size, *s*, distribution in the Y-direction of a weld of thickness, *t* (mm), is assumed to follow the normalized exponential distribution

$$P_{sg}(s,\lambda_s,t) = \frac{1 - e^{-\lambda_s s}}{1 - e^{-\lambda_s t}} \tag{1}$$

where

λ_s — flaw-size parameter

The probability-density function of the flaw-size parameter is

$$P_{\lambda s}(\lambda_s) = \frac{s_t^{n_f}}{\Gamma(n_f)} \lambda_s^{n_f - 1} e^{-\lambda_s s_t} \tag{2}$$

where

Γ — gamma function
s_t — sum of all flaw sizes
n_f — number of observed flaws

Because there is no gamma function on Microsoft® Office Excel (Microsoft Corporation, 2003) the gamma function Γ is calculated by inverting the natural log function

$$\Gamma = (\text{GAMMALN}(n_f)) = 720 \tag{3}$$

The value of Γ is calculated in cell B4 in file A1.xls. The increment of λ_s is specified in cell B1. The calculated probability-density function, $p_{\lambda s}(\lambda_s)$, is shown in column B as a function of the size parameters of column A.

With the size parameter in a distribution, the probability-density function of the flaw size is given by

$$p_{msg}(s,t) = \int_0^\infty \frac{\lambda_s e^{-\lambda_s s}}{1 - e^{-\lambda_s t}} p_{\lambda s}(\lambda_s) d\lambda_s \tag{4}$$

At a specified value of flaw size, *s,* the probability-density function is obtained by numerical integration. In file A2.xls, the size parameter is given in column A, and the integration is carried out in columns B and C. According to Bechtel SAIC Company, LLC (2004, Attachment I, Figure I.1), the value of $p_{\lambda s}(\lambda_s)$ is as small as 10^{-6} at $\lambda_s = 1$. Therefore, a value of $\lambda_s = 2$ is used as the upper limit of numerical integration in determining $p_{msg}(s,t)$. The resulting $p_{msg}(s,t)$ for a specified *s* is saved in cell C201.

In the file A2.xls, the flaw size, *s*, in cell B5 is used in the previously mentioned spreadsheet calculation. Once a value of *s* is entered in the cell B5, the calculation is carried automatically, and the resulting $p_{msg}(s,t)$ is saved in cell C201.

The cumulative-distribution function of flaw size is given by

$$P_{msg}(s,t) = \int_0^s p_{msg}(u,t)du \tag{5}$$

In file A2.xls, a Visual Basic code was written to check the previous calculation. In the code, the value of the flaw size, *s*, changes from *s0* in cell F2 to *s1* in cell F3 with increment *ds* in cell F1. The value of *s* is in column E. For each increment of integration, the value of *s* is copied to cell B5, and the resulting $p_{msg}(s,t)$ of cell C201 is used in the calculation. The cumulative-density function at this flaw size is saved in column F.

1.1 How To Use the Excel File A2.xls

Click the file name to open the file A2.xls and choose "Enable Macros." In cell F1, enter the desirable step size for integration, and in cell F3, enter the maximum flaw size to be examined. It is not necessary to set the smallest flaw size (let it be zero). Then, press ALT–F8; a window will pop up, which shows the Macro *test1*. Click the "RUN" button to execute the calculation. The results will automatically appear in the spreadsheet. The value of *s* is in column E, and the cumulative-distribution function at this flaw size is saved in column F.

1.2 Simplified Calculations (Excel File A3.xls)

The mean value of the flaw-size parameter is $\lambda_{sm} = n_f/s_t = 7/31.75 = 0.2205$ (cell B4). The cumulative-distribution function is given by Eq. (1) with λ_s being approximated by the mean value λ_{sm}

$$P_{sg}(s,\lambda_s,t) = \frac{1 - e^{-\lambda_{sm}s}}{1 - e^{-\lambda_{sm}t}} \tag{6}$$

The cumulative-distribution function of flaw size can be calculated, as shown in column B of A2a.xls. Every time the cells B1–B4 have a new value, the results of column B will be recalculated automatically. Note that the flaw size, s, is always smaller than the plate thickness, *t*.

In file A3.xls, the second curve (column C) is from file A2.xls, which gives higher accuracy.

2 FLAW DENSITY (EXCEL FILE A4.XLS)

The probability-density function for the flaw-density parameter, λ_d, is given by

$$p_{\lambda_d}(\lambda_d) = \lambda_d^{\,n_f - 0.5} e^{-\lambda_d L_t} \frac{L_t^{\,nf+0.5}}{\Gamma(n_f + 0.5)} \tag{7}$$

where L_t is the total ring length of the sample {= 77.6 m [254 ft]}. The gamma function is calculated by inversion of the natural log of the gamma function, GAMMALN.

The cumulative-distribution function for the flaw-density parameter, λ_d, is given by

$$P_{\lambda d}(\lambda_d) = \int_0^{\lambda_d} p_{\lambda d}(u)du \tag{8}$$

The Excel calculation of the cumulative-distribution function is shown in the file A4.xls.

3 FLAW ORIENTATION (EXCEL FILE A5.XLS)

In the reviewed document, the probability-density function of flaw orientation is assumed to follow a normal distribution

$$p_\theta(\theta,\sigma) = 2\frac{1}{\sigma\sqrt{2\pi}}exp(-\frac{1}{2}(\frac{\theta}{\sigma})^2) \tag{9}$$

where

σ — standard deviation

In Excel, the value of $p_\theta(\theta,\sigma)$ is calculated by using the function *NORMDIST* with a "*False*" argument for the normal distribution

$$p_\theta(\theta,\sigma) = 2 \times NormDist(\theta,0,\sigma,False) \tag{10}$$

The cumulative-distribution function is

$$P_\theta(\theta,\sigma) = 2\int_0^\theta \frac{1}{\sigma\sqrt{2\pi}}exp(-\frac{1}{2}(\frac{u}{\sigma})^2)du \tag{11}$$

because

$$P_\theta(\theta,\sigma) = 2\int_{-\theta}^{\theta} \frac{1}{\sigma\sqrt{2\pi}} \exp\left[-\frac{1}{2}\left(\frac{u}{\sigma}\right)^2\right]du - 2\int_{-\theta}^{0} \frac{1}{\sigma\sqrt{2\pi}} \exp\left[-\frac{1}{2}\left(\frac{u}{\sigma}\right)^2\right]du \tag{12}$$

In Excel, the cumulative-distribution function is calculated by using the function *NORMDIST* in the following way

$$P_\theta(\theta,\sigma) = 2 * [NormDist(\theta,0,\sigma,TRUE) - NormDist(0,0,\sigma,TRUE)] \tag{13}$$

The standard deviation, σ , of the normal distribution is evaluated by using the Bayesian approach with a noninformative prior. The probability-density function of σ is given by Bechtel SAIC Company, LLC [2004, Eq. (21)]. In the Excel file, the likelihood function is first calculated by the FUNCTION *lhf* in Visual Basic code. The input argument "s" is σ. The code is

```
Function lhf(s) As Double
Dim nf As Integer
Dim thetai(7) As Double
Dim pd As Double
Dim ic As Integer
nf = 7
thetai(1) = 0
thetai(2) = 2.6026
thetai(3) = 4.7636
thetai(4) = 5.7106
thetai(5) = 9.4623
thetai(6) = 14.0326
thetai(7) = 26.5651
lhf = 1
For ic = 1 To nf
' The following NORMIST needs "FALSE" to get pdf
pd = 2 * Application.WorksheetFunction.NormDist(thetai(ic), 0, s,
False)
lhf = lhf * pd
Next ic
End Function
```

The probability-density function of σ is then calculated by the FUNCTION pdfs. The code is

```
Function pdfs(s) As Double
' PDF of orientation parameter sigma
Dim ic As Integer
Dim si As Double
Dim dsi As Double
Dim dn As Double
Dim dnn As Double
Dim dno As Double
Dim nstep As Integer
'
' First, get the denominator by integration
nstep = 500
dsi = 0.1
si = 0.00000001
dn = 0
dnn = 0
For ic = 1 To nstep
dnn = lhf(si) / si
If (ic > 1) Then
dn = dn + 0.5 * dsi * (dnn + dno)
End If
si = si + dsi
dno = dnn
Next ic
'
'  Get the pdf for sigma
'
pdfs = (lhf(s) / s) / dn
'
End Function
```

In the Excel file, cell B1 is in increments of σ for numerical integration; B2 is the mean value of σ as calculated by

$$\sigma_m = \int_0^\infty \sigma p_\sigma(\sigma) d\sigma \tag{14}$$

The actual numerical integration is carried out on column E, and the result is in the end of the column (cell B2 = cell E502). The calculated value of σ_m = 13.82 is the same as that reported in the document.

The expected fraction of flaws, F_θ, that have an angle θ greater than the critical angle θ_c, is calculated using the following formula

$$F_\theta = \int_0^\infty [1 - P_\theta(\theta_c, \sigma)] p(\sigma) d\sigma \tag{15}$$

The critical angle θ_c is defined in cell B3. For a critical angle of 45°, the numerical calculation to obtain the cumulative-distribution function is carried out in columns F, G, and H. The result is posted in cell B4.

3.1 How To Use the Excel File A5.xls

(1) Choose a step size of σ in cell B1. Once chosen, the spreadsheet will recalculate automatically. However, it takes a while to complete the calculation. The progress of the calculation is shown in the lower left corner of the screen.

(2) Choose a critical angle θ_c in cell B1. Once chosen, the spreadsheet will recalculate automatically. However, it takes a while to complete the calculation.

4 ULTRASONIC CHARACTERIZATION (EXCEL FILE A6.XLS)

The functional forms are given by Bechtel SAIC Company, LLC [2004, Eqs. (21) and (22)]. The Excel calculations are straightforward. It is noted that the argument in the complementary-error function becomes negative when flaw size s is less than the characteristic size s_o. Because the argument x in the complementary-error function, ERFC(x), in Excel has to be nonnegative, it requires some treatment for the cases $s < s_o$. The complementary-error function is

$$erfc(x) = \frac{2}{\sqrt{\pi}} \int_x^\infty e^{-t^2} dt \tag{16}$$

For × < 0 (i.e., $s<s_o$),

$$\begin{aligned} erfc(x) &= \frac{2}{\sqrt{\pi}} \int_x^0 e^{-t^2} dt + \frac{2}{\sqrt{\pi}} \int_0^\infty e^{-t^2} dt = \frac{2}{\sqrt{\pi}} \int_0^{|x|} e^{-t^2} dt + \frac{2}{\sqrt{\pi}} \int_0^\infty e^{-t^2} dt \\ &= \frac{2}{\sqrt{\pi}} \left(\int_0^\infty e^{-t^2} dt + \int_{|x|}^\infty e^{-t^2} dt \right) + \frac{2}{\sqrt{\pi}} \int_0^\infty e^{-t^2} dt = 2erfc(0) - erfc(|x|) \end{aligned} \tag{17}$$

Bechtel SAIC Company, LLC [2004, Eqs. (21) and (22)] specifies the parameters in cells B1–B7, and the calculated results are in columns B, C, and D.

5 FLAW SIZE AFTER INSPECTION AND REPAIR (EXCEL FILE A7.XLS)

Bechtel SAIC Company, LLC [2004, Eqs. (23)–(26)] evaluates the flaw-size distribution after ultrasonic inspection and repair.

In the Excel file, the parameters are self-explanatory. The PND1 curve is based on a characteristic size of s_o = 2.5 mm [0.1 in]. The flaw size is given in column A. At a specified-size parameter, λ_s, in cell B6, the F_{ND} is calculated by numerical integration in column E and the value of F_{ND} is copied to cell E5 for later use. For a specified-size parameter, λ_s, in cell B6, the value of $P_{\lambda s}$ is calculated in cell E6.

The integration to determine the cumulative-distribution function in Bechtel SAIC Company, LLC [2004, Eq. (26)] is carried in columns H–K. In column I, the integrand in Bechtel SAIC Company, LLC [2004, Eq. (25)] is calculated at a specified λ_s and flaw size u. The actual integration over λ_s is carried in the subroutine pmsg. The value of p_{msgut} in Bechtel SAIC Company, LLC [2004, Eq. (26)] is shown in column K. A plot of cumulative-distribution function (column K) versus the flaw size is shown. By using the data, the average flaw-size is calculated as 1.33 mm [0.05 in] (column L), compared to the 1.3 mm [0.05 in] reported by Bechtel SAIC Company, LLC (2004). This discrepancy is caused by the large step size in the present calculation.

```
Sub pmsg()
Dim i As Integer
Dim j As Integer
Dim istep As Integer
Dim ds As Double
Dim s As Double
Dim s0 As Double
Dim s1 As Double
Dim prob As Double
Dim u As Double
Dim du As Double
Dim t As Double
Dim value As Double

ds = Cells(1, 9).value
s0 = 0.001
s1 = Cells(2, 9).value
istep = (s1 - s0) / ds + 1

t = Cells(7, 2).value
du = Cells(1, 2).value
jstep = t / du
u = 0

For j = 1 To jstep
u = u + du
s = s0
prob = 0
'
'
```

```
For i = 1 To istep

'assign lambda
'
Cells(6, 2).value = s
value = Cells(11 + j - 1, 9).value
'
'Cells(11 + i - 1, 9).Value = s
prob = prob + ds * value
If i = 1 Then
prob = prob - 0.5 * ds * value
End If
If i = istep Then
prob = prob - 0.5 * ds * value
End If
s = s + ds
Next i
'
Cells(11 + j - 1, 10).value = prob
Next j

End Sub
```

5.1 How To Use the Excel File A7.xls

Click the file name to open the file A7.xls and choose "Enable Macros." Specify a step size of *s* in cell B1 and other parameters. Once chosen, some parts of the spreadsheet will recalculate automatically. To activate the MACRO (for subroutine pmsg), press ALT–F8; a window that shows the Macro *test1* should pop up. Click the "RUN" button to execute the calculation. The results will automatically show in the spreadsheet. However, it takes a long while to complete the calculation. The progress of the calculation is shown in the lower left corner of the screen.

6 FLAW DENSITY AFTER INSPECTION AND REPAIR (EXCEL FILES A8.XLS AND A9.XLS)

Bechtel SAIC Company, LLC [2004, Eq. (28)] evaluates the flaw-density parameter, λ_{utd}, after ultrasonic inspection and repair. There are two variables, the density parameter, λ_d, and size parameter, λ_s. Both of these parameters have their own distribution functions. The approach to evaluate the distribution function of the density parameter, λ_{utd}, is based on the Latin Hypercube sampling technique developed by McKay, et al. (1979).

The basic concept is to sample sets of independent variables whose space is predivided into intervals of equal probability. For the present case of λ_{utd}, the space of density parameter, λ_d, and the size parameter, λ_s, are divided into n_s intervals. For the present calculation, n_s is chosen to be 1,000, although 2,000 was used in the document. In order to subdivide the space of λ_d and λ_s into 1,000 intervals of equal probability. The cumulative-distribution function is calculated for each of these intervals (i.e., the Y-axis of the cumulative-distribution function chart is divided into 1,000 intervals, and the corresponding interval in the abscissa would have the same probability). This procedure applies to both λ_d and λ_s. In the file A8.xls, columns Q and R register the intervals in the Y-axis (cumulative-distribution function). Within each cumulative-distribution function interval, a random number, u_i, is chosen. Each of these u_i corresponds to a value of λ_d or λ_s. Altogether, there are an n_s number of sampled u_{di} and u_{si}

whose probability is equal. Columns S (size) and T (density) are created by a random number generator, *dRandReal* of PopTool (an Excel Add-in module).

The next step is to sample the pair of λ_s and λ_d in order to evaluate the parameter λ_{utd}. This is done by randomly sampling the columns S and T; the resulting columns are U and V. Each row of these two columns then becomes a sample set of u_{si} and u_{di} for λ_s and λ_d, respectively. The actual values of λ_s and λ_d, corresponding to each u_{si} and u_{di}, are obtained by linear interpolation from the cumulative-distribution function curve.

The value of λ_s is in column L, and the cumulative-distribution function is in column N. The F_{ND} in Bechtel SAIC Company, LLC [2004, Eq. (23)], corresponding to each $_s$, is also calculated and placed in column O by using subroutine FND1.

The value of λ_d is in column A, and the cumulative-distribution function is in column D.

In column X, the cumulative-distribution function of the corresponding λ_s in column U is interpolated. In column Y, the cumulative-distribution function of the corresponding λ_d in column V is interpolated. The interpolation is carried out by using the subroutine INTE. A special technique is used in the subroutine to execute the integration successfully (see the subroutine INTE). A similar procedure is used to interpolate the F_{ND} in column Z. After this, the flaw-density parameter, λ_{utd}, after ultrasonic inspection and repair is calculated by Bechtel SAIC Company, LLC [2004, Eq. (28)]. The result is in column AA; each λ_{utd} corresponds to a pair of λ_s and λ_d whose probability is uniformly random.

The Visual Basic code of the subroutine INTE is

```
      Sub inte()
          Dim i As Integer
          For i = 1 To 1000
'
' Remarks:
'
    ww = "w" & i
    ww1 = ww & i
'   ww1 becomes w11, w22, w33 etc
'
u = "u" & i
arg = "=Interpolate(" & u & ", N11:N111, L11:L111)"
Cells(i, 24).Formula = arg
'
v = "v" & i
arg = "=Interpolate(" & v & ", D7:D107, A7:A107)"
Cells(i, 25).Formula = arg
    Next i
End Sub
```

There are 1,000 data points of λ_{utd}. The column is copied to column A in the file A9.xls. To construct the cumulative-distribution function chart, the column is first sorted. Then, the histogram in the data analysis is used to obtain the probability-density function of λ_{utd} (columns B and C). The cumulative-distribution function is obtained by simple integration of the

probability density function, as saved in column D (in total count) and E (in fraction). The mean, λ_{utd}, is calculated by

$$\lambda_{mutd} = \frac{1}{n_s} \sum \lambda_{utd} \tag{18}$$

The calculated value of λ_{mutd} is 0.0396 flaw/m [0.0121 flaw/ft], which differs only slightly from the value of 0.0407 flaw/m [0.0124 flaw/ft] reported in the document. Bear in mind that the spreadsheet A8.xls uses a random-number generator. The code recalculates and changes the results every time the file is opened, and some cells are specified with new values.

7 REFERENCES

Bechtel SAIC Company, LLC. "Analysis of Mechanisms for Early Waste Package/Drip Shield Failure." CAL–EBS–MD–000030. Rev. 00C ICN 00. Las Vegas, Nevada: Bechtel SAIC Company, LLC. 2004.

McKay, M.D., W.J. Conover, and R.J. Beckman. "A Comparison of Three Methods for Selecting Values of Input Variables in the Analysis of Output From a Computer Code." *Technometrics*. Vol. 221. pp. 239–245. 1979.

Microsoft Corporation. "Microsoft® Office Excel 2003." Redmond, Washington: Microsoft Corporation. 2003.